A comparative study of poly(methyl methacrylate) and polystyrene/clay nanocomposites prepared in supercritical carbon dioxide

Qian Zhao [a], Edward T. Samulski [a,b,*]

[a] *Curriculum in Applied and Materials Sciences, University of North Carolina at Chapel Hill, Chapel Hill, NC 27599 3290, USA*
[b] *Department of Chemistry, University of North Carolina at Chapel Hill, CB#3290, Chapel Hill, NC 27599 3290, USA*

Abstract

Poly(methyl methacrylate) and polystyrene/clay nanocomposites have been prepared via pseudo-dispersion polymerizations in the presence of a poly(dimethylsiloxane) surfactant-modified clay (PDMS-clay) in supercritical carbon dioxide. The effects of the PDMS-clay concentration on polymer conversion, molecular weight, and morphology have been investigated. The insoluble dispersion of PDMS-clay is shown to be an effective stabilizer for both MMA and styrene polymerization in scCO$_2$. The nanocomposites were characterized by X-ray diffraction (XRD), transmission electron microscopy (TEM), thermogravimetric analysis (TGA), and dynamic mechanical analysis (DMA). While XRD shows featureless patterns for both nanocomposites, the actual distributions of clay are found to be quite different between PMMA and PS nanocomposites, presumably due to the different interaction mechanisms between the polymers and clay. Consequently, the different states of clay in the two nanocomposites play an important role in the mechanical properties of the nanocomposites, and a to a lesser degree in the thermal properties.
© 2005 Elsevier Ltd. All rights reserved.

1. Introduction

Polymer/clay nanocomposites in which a small percentage of layered silicates are embedded in a polymer matrix are of interest because they exhibit enhanced material properties compared to the neat polymer [1]. Among various approaches used to prepare nanocomposites, in situ polymerization has proved to be the most successful one, pioneered by researchers from Toyota Motor Company who synthesized the first exfoliated nylon-6/clay hybrid for automotive applications [2]. Since then, several useful vinyl polymer/clay nanocomposites have been prepared via in situ polymerization, such as poly(methyl methacrylate) (PMMA) and polystyrene (PS) nanocomposites [3,4]. In order to render clay organophilic and more compatible with organic polymers, the sodium ions of the pristine clay are usually replaced with an alkylammonium surfactant via an ion exchange reaction. By using two different organically modified clays, Wang and coworkers prepared

poly(methyl methacrylate)/clay nanocomposites and polystyrene/clay nanocomposites via bulk, solution, suspension and emulsion polymerization [5]. Both exfoliated and intercalated nanocomposites were obtained, depending on the organic treatments of clay as well as the particular preparative method that was used. The exfoliated nanocomposites exhibited superior thermal stabilities and mechanical properties compared to the pure polymers, generally attributed to the uniform dispersion of clay silicate layers in the polymer matrix. However, a drawback of in situ polymerization is that it typically involves large quantities of aqueous/organic solvents which are both environmentally unfriendly and economically prohibitive for an industrial-scale application.

On the other hand, supercritical carbon dioxide (scCO$_2$) has attracted extensive interest as a polymerization and processing medium, primarily driven by the need to replace conventional solvents with more environmentally benign and economically viable systems [6]. One area of interest has been the dispersion polymerization of vinyl monomers, which has been pioneered by DeSimone et al., who reported the first dispersion polymerization of methyl methacrylate in scCO$_2$ [7]. Because the product, poly(methyl methacrylate) is insoluble in scCO$_2$, they used a CO$_2$-soluble fluorinated homopolymer (poly(dihydroperfluorooctyl acrylate) PFOA) as the stabilizer for the polymerization system. Consequently, the successful dispersion

polymerization led to a significant improvement in the yield, molecular weight and morphology of the resultant polymer.

Typically, an effective stabilizer for CO_2 polymerizations should have two prerequisites: (1) an anchoring segment which attaches to the monomer/polymer particle either through physical adsorption or chemical grafting; (2) a CO_2-philic (fluorinated- or siloxane-based) segment which projects into the continuous CO_2 phase and provides steric stabilization for the growing polymer particles. Many sophisticated stabilizers ranging from fluorinated and siloxane-based block or graft copolymers [8–10], siloxane-based macromonomers [11], to more recent monofunctional perfluoropolyethers [12] have been utilized.

Recently, Zerda et al. used the in situ polymerization route to prepare highly filled PMMA/clay nanocomposites in scCO_2 [13]. In their work, CO_2 was primarily used to lower the viscosity resulting from high loadings (up to 40%) of clay; the clay was modified by conventional hydrocarbon surfactants and resulted in intercalated PMMA/clay nanocomposites. More recently, Dong and coworkers employed a similar in situ polymerization technique to prepare intercalated PS/clay nanocomposites with a more conventional loading (1–10%) of clay in scCO_2 [14]. They also modified clay with a hydrocarbon surfactant and found that a longer 'soaking time' during the impregnating process can lead to more exfoliated nanocomposites. Nevertheless, in both studies, no information on the yields or morphologies of the polymers has been mentioned, nor was it clear why in situ polymerization with clay can produce nanocomposites in higher yields while polymerizations in the absence of stabilizer typically result in a non-descriptive, low-yield oligmer in scCO_2 [7]. Furthermore, by using hydrocarbon surfactant-modified clay in the two studies, only intercalated nanocomposites have been obtained regardless of the concentration of clay.

We recently reported a route to produce partially exfoliated poly(methyl methacrylate)/clay nanocomposites via in situ polymerization in scCO_2, in which we found that the fluorinated surfactant-modified clay can itself serve as a stabilizer and help produce PMMA in high yields in scCO_2 [15]. Although the clay is not soluble in CO_2, the stabilization mechanism is similar to that in a conventional dispersion polymerization; FT-IR results indicated hydrogen bond formation between the carbonyl group of the MMA monomer and hydroxyl groups and/or interlayer water of the clay. We referred to this technique as a pseudo-dispersion polymerization. In this paper, we report the use of a different system, a commercially-available surfactant aminopropyl-terminated poly(dimethylsiloxane) (AP-PDMS) modified clay as the stabilizer for the pseudo-dispersion polymerization of methyl methacrylate and styrene in scCO_2. This PDMS-based surfactant is known to be CO_2-philic and its longer siloxane chain is expected to provide better steric stabilization compared to the shorter fluorinated chain used previously. Furthermore, we extend our system to polystyrene (PS), which does not have a hydrogen bonding site as PMMA does. Having different interaction mechanisms with clay, PMMA and PS are two model systems that allow us to study the effects of a clay-based stabilizer on both hydrogen-bonding polymers (e.g. PMMA) and non-hydrogen-bonding polymers (e.g. PS). In this paper, the effects of PDMS-clay on the morphologies and properties of PMMA and PS nanocomposites are compared. Two stabilization mechanisms are proposed to account for the different microstructures and mechanical properties between PMMA and PS nanocomposites.

2. Experimental

2.1. Materials

Sodium montmorrillonite (Na-MMT) was obtained from Gelest, Inc and used as received. Dimethyldistearylammonium bromide were supplied by TCI America and used as received. Aminopropyl-terminated poly(dimethylsiloxane) ($M_w = 3500$, structure shown in Fig. 1) was obtained from United Chemical Technologies, Inc. Methyl methacrylate and styrene were purchased from Aldrich Chemical Company and purified by distillation before use. The free radical initiator, 2,2-azobis(isobutyronitrile) (AIBN) was supplied by Polysciences, Inc. PMMA ($M_w = 350$ kDa) and PS ($M_w = 150$ kDa), used as controls, were obtained from Aldrich Chemical Company.

2.2. Modification of clay

Aminopropyl-terminated poly(dimethylsiloxane) was acidified with hydrochloric acid in tetrahydrofuran (acidification ratio = 1/2). The cation exchange procedure was followed using previously described methods [16]. The resultant organo-clay was obtained as a yellowish sticky solid, and was denoted 'PDMS-clay'. For comparison, we also modified the clay with a hydrocarbon surfactant dimethyldistearylammonium bromide. The modified clay is comparable to a commercially-used clay (Cloisite 20A from Southern Clay) and was denoted '2C18-clay'. The organic content in PDMS-clay and 2C18-clay was determined to be 65 and 40% respectively, according to thermogravimetric analysis.

2.3. Polymerization

Polymerizations were conducted in CO_2 in a 2.5 ml, high-pressure cell equipped with sapphire windows that allow visual observation of the mixture. In a typical polymerization, the initiator AIBN and PDMS-clay were weighed into the cell containing a magnetic stir bar. The cell was purged with CO_2 via an Isco automatic syringe pump (Model 260D) for a few minutes; then the monomer was injected into the cell. The cell was then filled with CO_2 to 70 bar, and heated to 65 °C. After the desired temperature was reached, the desired pressure was
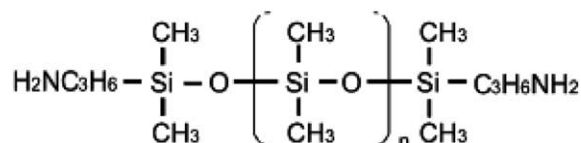

Fig. 1. Aminorpropyl-terminated PDMS (AP-PDMS, $n \sim 44$).

achieved by the addition of more CO_2. The reaction was allowed to proceed with stirring for a specific time, and then the cell was cooled and the CO_2 was slowly vented. Unless specified, the final product was taken out and dried at room temperature in a vacuum oven overnight, and the resultant materials stored in a desiccator for characterization. Yields of the polymer were determined gravimetrically. For dynamical mechanical analysis, the composite was heated in a vacuum oven at 150 °C overnight to remove residual CO_2 trapped within the polymer. The sample was then pulverized and compression molded (180 °C, 54 MPa) into a thin plaque.

2.4. Characterization

Powder X-ray diffraction (XRD) data ($2\theta = 2$ and $10°$) were collected on a Rigaku multiflex diffractometer using Cu K$_\alpha$ radiation (40 kV, 40 mA) at a scan rate of 0.5°/min. Scanning electron microscopy (Hitachi S-4700 FE-SEM) and transmission electron microscopy (TEM) (Phillips CM12) were used to investigate the morphologies and microstructures of the nanocomposites. Samples for SEM were mounted on aluminum stubs using an adhesive carbon tab, then gold coated. Samples for TEM were either directly from the powdery sample or cut from the compression-molded sample. The samples were embedded and cured in epoxy resin and thin-sectioned using an ultramicrotome (Reichert Supernova) equipped with a diamond knife. Thermogravimetric analysis (TGA) was performed using a Perkin–Elmer Pyris 1 TGA system in an argon atmosphere at a heating rate of 10 °C/min. The storage modulus and glass transition temperature of the PMMA nanocomposites were measured by a dynamic mechanical analyzer (Perkin–Elmer DMA 7e) using a extension measuring system operating at a frequency of 1 Hz; measurements were conducted in the air from room temperature to 140 °C at a scan rate of 5 °C/min. Molecular weights of filtered polymers were obtained by gel permeation chromatography (GPC) using Waters microstyragel columns (pore size 10^5, 10^4, and 10^3 Å) and differential refractometry (Waters model 410) detector. Polystyrene standards were used for calibration.

3. Results and discussion

3.1. Synthesis

The pseudo-dispersion polymerizations of MMA were conducted with 0.5 ml MMA monomer at concentrations of 6 wt% PDMS-clay (with respect to monomer) and 0.6 wt% AIBN (with respect to monomer) at 65 °C, 241 bar for 4 h in a 2.5 ml CO_2 cell. The pseudo-dispersion polymerizations of styrene were conducted with 0.5 ml styrene monomer at concentrations of 7 wt% PDMS-clay (with respect to monomer) and 1 wt% AIBN (with respect to monomer) at 65 °C, 344 bar for 48 h in a 2.5 ml CO_2 cell. Unlike typical dispersion polymerizations in which reactions start out homogeneously with a stabilizer soluble in the CO_2 phase, the pseudo-dispersion polymerizations were heterogeneous throughout the reaction. Although clay is not soluble in CO_2, the PDMS-modified clay formed a milk-like suspension under magnetic stirring. As the reaction proceeded, the suspension appeared to thicken, and precipitated powder accumulated on the windows. Upon venting CO_2 at the end of the reaction, a white dry powder was recovered in the form of fine particles. The yield of PMMA was 88% with M_w 450 kDa (entry 2 in Table 1); the yield of PS was 93% with M_w 126 kDa (entry 8 in Table 1). These high conversions and high molecular weights of polymers indicate successful dispersion polymerizations in CO_2.

3.2. Effect of PDMS-clay concentration on polymerization of MMA

Analysis by SEM shows that the precipitated PMMA/PDMS-clay nanocomposites primarily consist of spherical PMMA particles (Fig. 2(a)) with an average particle diameter about 10 μm. These particles show a relatively broad size distribution, presumably due to the ill-defined interaction mechanism between the monomers and insoluble clay platelets as compared to the typical, molecular interactions between monomers and soluble (polymeric) surfactants. Nevertheless, as the concentrations of PDMS-clay increase from 6 to 11 and 20%, the average diameter of the PMMA particles decreases

Table 1
Pseudo-dispersion polymerizations of MMA and styrene in scCO$_2$

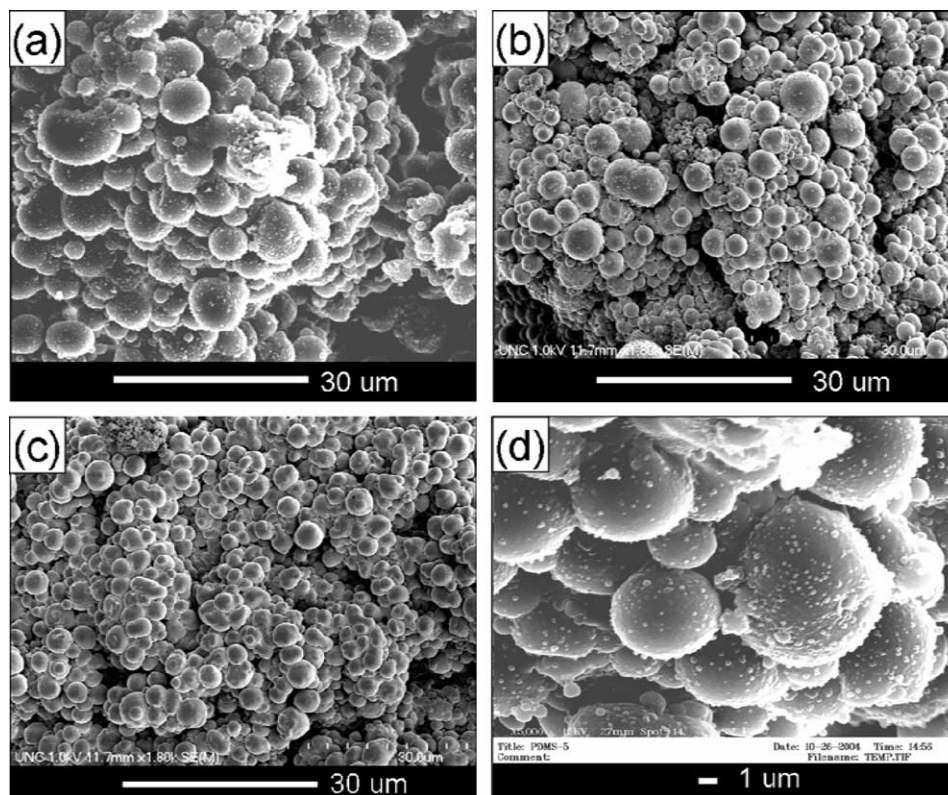|	Entry	PDMS-clay (%)	2C18-clay (%)	Yield (%)	M_w (kDa)	Sample description
PMMA	1	4		57	381	Aggregated powder
	2	6		88	450	Fine powder
	3	9		85	524	Fine powder
	4	11		87	590	Fine powder
	5	20		96	367	Fine powder
	6		6	38	392	Aggregated powder/flake
PS	7	5		75	114	Viscous block
	8	7		93	126	Fine powder
	9	13		95	109	Fine powder
	10	23		88	79	Fine powder
	11		6	77	138	Aggregated powder/block

Fig. 2. SEM images of PMMA/PDMS-clay nanocomposites with varying PDMS-clay concentration: (a) 6%, (b) 11% and (c) 20%; (d) higher magnification SEM image of PMMA/PDMS-clay nanocomposites with 6 wt% PDMS-clay.

and becomes more uniformly distributed, as shown in Fig. 2(a)–(c). This is consistent with a typical dispersion polymerization in $scCO_2$ and indicative of a more efficient stabilization of smaller particles with increasing stabilizer concentration. In addition, the molecular weights of PMMA increased with increased PDMS-clay concentration until the PDMS-clay concentration reaches 11% (Table 1). For comparison, an identical polymerization of MMA was conducted with the 2C18-clay as the stabilizer. As shown in entry 6 in Table 1, the relatively low yield (38%) and irregular morphologies of the resulting PMMA indicate the poor stabilizing ability of the hydrocarbon surfactant-modified clay in CO_2 relative to the PDMS-clay; the hydrocarbon surfactant is not CO_2-philic and cannot provide good steric stabilization for the monomer/polymer particles in $scCO_2$.

An interesting observation for PMMA with 6% PDMS-clay is that there are many small particles on the surface of primary PMMA particles (Fig. 2(d)). Clay platelets are irregular in shape however these small particles seem to be round and smooth, so we can exclude the possibility that these coordinated small particles are clay platelets. Instead, we believe that these small particles are secondary PMMA particles, and the formation of this interesting morphology can be attributed to the difunctional aminopropyl groups in the AP-PDMS surfactant. As is depicted in Fig. 3, we have proposed previously that the stabilization mechanism is most likely steric stabilization in the CO_2 phase with the clay itself interacting with the carbonyl group of the methacrylate moiety

via H-bonding [15]. In our current system, although one end of aminopropyl group has been quaternized and attached to the cation exchange site of clay, the other end may still interact with the carbonyl group of MMA monomer via a H-bond and serve as a secondary anchoring point for PMMA growth. Actually, it has been reported by Okubo and coworkers that AP-PDMS alone can stabilize dispersion polymerization of MMA in $scCO_2$ [17]. Since it is known that primary aliphatic amines react with CO_2 to form carbamic acid [18], they proposed that the interaction between AP-PDMS and MMA can be either hydrogen bonding between the carbamic acid group and the carbonyl group, or hydrogen bonding between the aminopropyl group and the carbonyl group.

3.3. Effect of PDMS-clay concentration on the polymerization of styrene

Again, in the case of PS/PDMS-clay nanocomposites, increasing the concentration of PDMS-clay also results in a decrease in composite particle diameter and a narrower size distribution (Fig. 4(a)–(c)). In contrast, the morphology of the PS/2C18-clay nanocomposite is ill-defined (Fig. 4(d)) and the yield is low (entry 11 in Table 1). Clearly the PDMS-clay is also acting as a stabilizer for styrene polymerization, although there is no hydrogen bond between styrene and clay as in the MMA-clay system. Styrene merely interacts with clay through a weak van der Waals interaction. This much weaker interaction is evidenced by a much longer polymerization
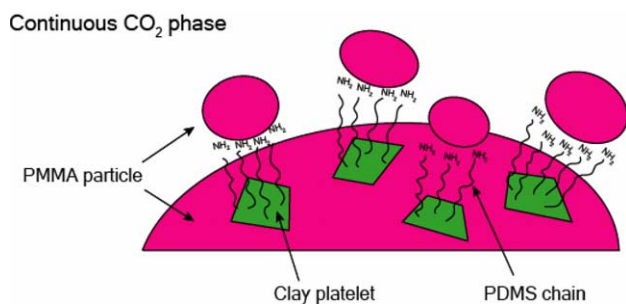
Fig. 3. Schematic illustration of a primary PMMA particle (shown in red) stabilized by PDMS-clay in which the clay platelet (shown in green) acts as a primary anchor and the aminopropyl group on the free end of the PDMS chains serves as a secondary anchor for the small PMMA particles (shown in red) (For interpretation of the reference to colour in this legend, the reader is referred to the web version of this article).

time (>40 h) to reach high polymer conversion than conventional dispersion polymerizations of styrene in scCO$_2$ (24–40 h) [8,19,20]. In addition, the molecular weights of PS do not change much with increases in the PDMS-clay concentration (Table 1). However, the van der Waals interaction is clearly capable of bringing styrene into the clay gallery and providing sufficient anchoring to help produce PS in high yields in scCO$_2$. Additional proof that there must be an anchoring interaction between styrene and clay comes from a comparison with dispersion polymerization using the AP-PDMS surfactant alone. Although AP-PDMS has been shown to act as a stabilizer and help stabilize MMA polymerization in scCO$_2$, it was observed that in the case of styrene

polymerization, no stabilized polymerization was obtained. With AP-PDMS alone, the polymerization of styrene resulted in a viscous liquid and an undesirably low yield, which is very similar to what is obtained in the complete absence of any stabilizer. This further confirms that there is no hydrogen bonding interaction between styrene and AP-PDMS and styrene must interact with clay to provide the necessary anchoring.

3.4. Comparison of XRD results of the PMMA and PS nanocomposites

X-ray diffraction (XRD) was used to characterize the layered structure of the polymer/clay nanocomposites. Fig. 5 shows the XRD patterns of the organoclays and PMMA and PS nanocomposites with PDMS-clay and 2C18-clay. As is seen from curves a and b, the basal spacings of 2C18-clay and PDMS-clay are found to be 3.9 and 7.1 nm respectively, based on their diffraction peaks in the pattern (The (001) diffraction peak of PDMS-clay is not shown in the pattern, but can be calculated from the higher order diffraction peaks in the pattern). It is reasonable that PDMS-clay has a larger d-spacing than 2C18-clay, since the length of PDMS surfactant ($n \sim 44$) is much longer than that of 2C18-surfactant. For PMMA and PS nanocomposites with 6 wt% 2C18-clay (curves c and d), the (001) peaks are almost unchanged from that of 2C18-clay, indicating that both nanocomposites are intercalated. These results are in agreement with what has been observed in previous studies [13,14]. In PMMA and PS nanocomposites
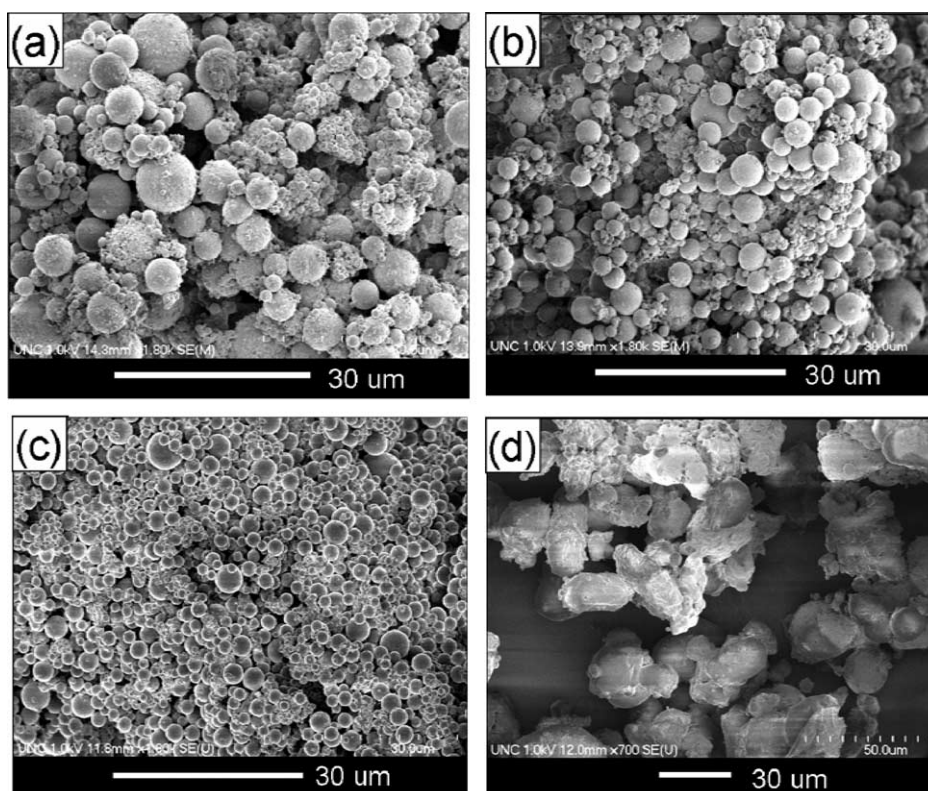

Fig. 4. SEM images of PS/PDMS-clay nanocomposites with varying PDMS-clay concentration: (a) 7%, (b) 13% and (c) 23% (d) SEM image of PS/2C18-clay nanocomposites with 6 wt% PDMS-clay.
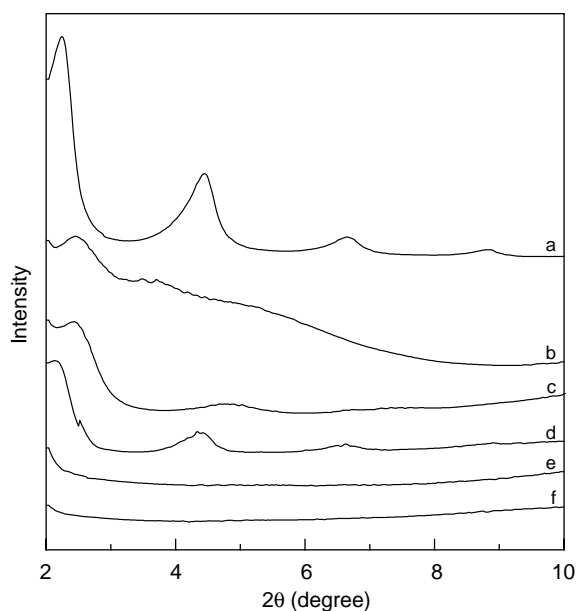
Fig. 5. XRD pattern of (a) 2C18-clay; (b) PDMS-clay; (c) PMMA nanocomposite with 6 wt% 2C18-clay; (d) PS nanocomposite with 6 wt% 2C18-clay; (e) PMMA nanocomposite with 6 wt% PDMS-clay; (f) PS nanocomposite with 7 wt% PDMS-clay.

with PDMS-clay, the characteristic peak disappears in the pattern, as shown in curves e and f, suggesting that the d-spacings of clay in the nanocomposites are larger than 4 nm, the detection limit of the instrument used in this study. The featureless patterns suggest that clay is nearly completely exfoliated in both polymers.

3.5. Comparison of TEM results of the PMMA and PS nanocomposites

More information about the microstructures of PMMA/PDMS-clay (6 wt% PDMS-clay) and PS/PDMS-clay (7 wt% PDMS-clay) nanocomposites was obtained by TEM observations. In the powdery PMMA/PDMS-clay nanocomposites shown in Fig. 6(a) and (b), the dark line represents individual silicate layers, whereas the brighter area represents the PMMA matrix. It can be seen that the silicate layers of clay have been completely exfoliated and uniformly dispersed in the PMMA matrix. This further supports the XRD analysis which suggests that exfoliated nanocomposites were formed. While for the powdery PS/PDMS-clay nanocomposites, as shown in Fig. 6(c), many dark, distinct spherical particles are distributed in the micrograph. These dark particles are actually PS particles, the size and distribution of which agree well with the SEM observations in the previous study. The observation of these darker PS particles can be attributed to the stronger electron scattering of PS relative to the epoxy resin, which scatters electron much weaker therefore appears to be lighter in the TEM. Since the contrast between PMMA and epoxy is not as distinct as that between PS and epoxy, PMMA particles cannot be readily distinguished in TEM. The brightest areas

are voids, which are probably formed as PS particles are ripped off the epoxy resin during sample sectioning. Surprisingly, the silicate layers in the PS nanocomposites are not distributed randomly and uniformly throughout the PS particle matrix as in the PMMA matrix. Instead, it can be seen that the darkest silicate layers are for the most part located on the exterior surfaces of the PS particles, manifested by the contrasting electron densities in Fig. 6(d). Clearly, the silicate layers are exfoliated into individual layers, or they consist of at most a few silicate sheets, as suggested by both TEM and XRD. However, when the powdery sample is compression molded into a continuous film, TEM reveals that these exfoliated silicate layers have re-aggregated together and formed stacks, as shown in Fig. 6(e). This phenomenon of re-aggregation is not unexpected, since the concentration of silicate layers on the exterior surfaces of neighboring PS particles makes possible a large number of contacts between silicate exterior layers on different PS particles. There is a kind of nanophase separation into silicate rich 'boundaries' wherein the clay is no longer exfoliated in the compression molded PS/PDMS-clay nanocomposite.

3.6. Comparison of thermal properties of the PMMA and PS nanocomposites

The thermal stabilities of both nanocomposites and polymers were studied by TGA analysis. Fig. 7(a) and (b) shows the TGA curves (the residual weight percentage versus temperature) and DTG curves (derivative of the residual weight percentage versus temperature) for PMMA/PDMS-clay nanocomposites and pure PMMA. Evidently, the decomposition onsets of PMMA/PDMS-clay nanocomposites shift to higher temperatures compared to that of pure PMMA. As shown in Fig. 7(b), pure PMMA appears to have two degradation steps at 288 and 333 °C, which were generally attributed to scissions at the chain-end initiation from vinylidene ends and random internal scission of the polymer chain, respectively [21]. While for PMMA/PDMS-clay nanocomposites, it can be seen that the first degradation step (288 °C) is largely depressed whereas the second degradation temperature is delayed by about 19 °C from that of pure PMMA. Therefore, it is apparent that the presence of clay stabilizes both steps of degradation, though further increase in clay concentration from 6 to 11% does not seem to affect decomposition temperature much. TGA and DTG curves for PS/PDMS-clay nanocomposites and pure PS are shown in Fig. 7(c) and (d). As seen in Fig. 7(d), the temperature at maximum degradation rate increases largely from 369 °C for pure PS to 398 °C for PS nanocomposites with 7 wt% clay and to 419 °C for PS nanocomposites with 13 wt% clay. Although clay is known to be concentrated on the exterior surfaces of PS particles, it seems that the presence of clay still plays an important role in enhancing the thermal stabilities of PS, by hindering the out-diffusion of the volatile decomposition products.
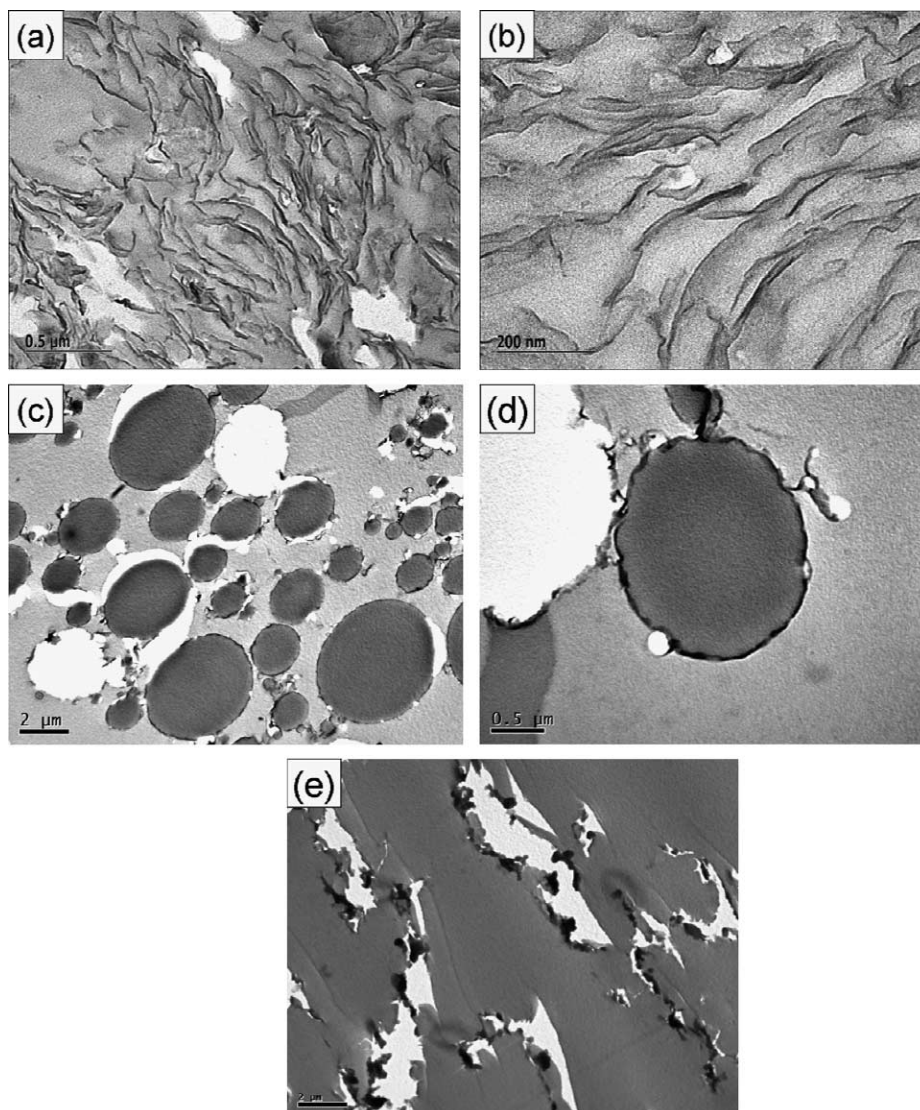
Fig. 6. TEM images of (a) powdery PMMA/PDMS-clay nanocomposite at low magnification image; (b) powdery PMMA/PDMS-clay nanocomposite at high magnification; (c) powdery PS/PDMS-clay nanocomposite; (d) compression molded PS/PDMS-clay nanocomposite.

3.7. Comparison of mechanical properties of the PMMA and PS nanocomposites

Dynamic mechanical analysis (DMA) was used to measure the viscoelastic properties of the polymer nanocomposites. Fig. 8 shows the temperature dependence of storage modulus and tan δ of PMMA and PMMA/PDMS-clay nanocomposites with 6 wt% PDMS-clay. As expected, the storage modulus of the PMMA nanocomposites increases compared to that of pure PMMA. A slightly-enhanced glass transition temperature ($T_g = 125\,^{\circ}$C for the nanocomposites versus $T_g = 122\,^{\circ}$C for pure PMMA) corresponding to the peak of the loss tangent is also observed for the PMMA/PDMS-clay nanocomposites. It has been suggested [22,23] that the enhancements of the storage modulus and glass transition temperature result from the strong interfacial interactions between the polymer and clay, the restricted segmental motions of polymer chains at the organic–inorganic interface, and the inherent high modulus of the clays. In our previous study, we synthesized PMMA nanocomposites with a fluorinated surfactant-modified clay (10F-clay), and also observed a increase in glass transition temperature over pure PMMA by 8 $^{\circ}$C [15]. Here, it should be noted that the increase in T_g for PMMA/PDMS-clay nanocomposites is only 3 $^{\circ}$C. This is probably due to the dual role organoclay plays in the nanocomposites: on one hand, it serves as an nano-filler leading to the increase in T_g and storage modulus; on the other hand, it is a plasticizer leading to the decrease in T_g and modulus [24]. Here, the longer PDMS chain may have a larger plasticizing effect than the fluorinated surfactant, which may be the reason why the PMMA/PDMS-clay nanocomposites have a slightly smaller increase in T_g compared to PMMA/10F-clay nanocomposites. As for PS/ PDMS-clay nanocomposites, we have been unable to perform dynamic mechanical analysis because the samples are too brittle. In conjunction with TEM observations, it is possible that the re-aggregation of clay in the compression molded
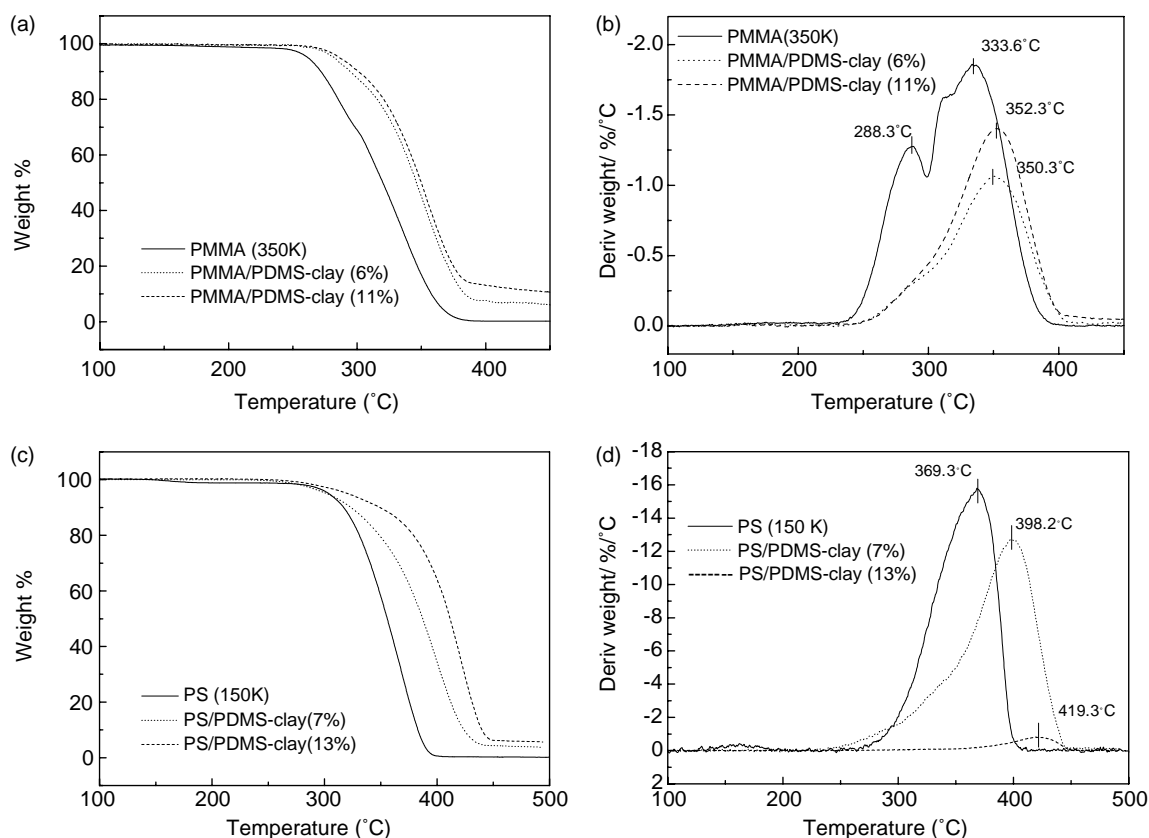
Fig. 7. (a) TGA curves of PMMA and PMMA/PDMS-clay nanocomposites; (b) DTG curves of PMMA and PMMA/PDMS-clay nanocomposites; (c) TGA curves of PS and PS/PDMS-clay nanocomposites; (d) DTG curves of PS and PS/PDMS-clay nanocomposites.

sample contributes to brittle nanophase-separated inorganic 'grain boundaries' in the PS nanocomposites. However, further study is needed to confirm this hypothesis.

4. Conclusions

PMMA/PDMS-clay and PS/PDMS-clay nanocomposites have been synthesized with high yields via a pseudo-dispersion polymerization technique in scCO$_2$. It has been found that insoluble PDMS-clay dispersions are an effective stabilizer for polymerizations of methyl methacrylate and styrene in scCO$_2$.

Fig. 8. Storage modulus and loss tangent (tan δ) spectra of PMMA and PMMA/PDMS-clay nanocomposites.

The morphologies of PMMA and PS depend strongly on the concentration of PDMS-clay, as anticipated for a conventional stabilizer. Whereas XRD results show featureless patterns for both PMMA and PS nanocomposites, TEM studies suggest that the distribution of clay are quite different in the two nanocomposites. In the case of the PMMA/PDMS-clay nanocomposites where the interaction between PMMA with clay is via hydrogen bonding, the silicate layers are completely exfoliated and uniformly dispersed in the PMMA matrix. While for PS/PDMS-clay nanocomposites where PS interacts with clay via a weaker van der Waals interaction, the silicate layers are exfoliated but concentrated mostly on the exterior surfaces of PS particles. As a result, the silicate layers of clay re-aggregate in the PS matrix after compression molding. Both PMMA and PS nanocomposites show enhanced thermal stabilities compared to the pure polymers, whereas the different distributions of clay seem to play an important role in mechanical properties of the nanocomposites. In general, the pseudo-dispersion polymerization route allows for clean synthesis of nanocomposites with high yields in scCO$_2$, without the need for adding extra surfactant to stabilize the polymerization system.
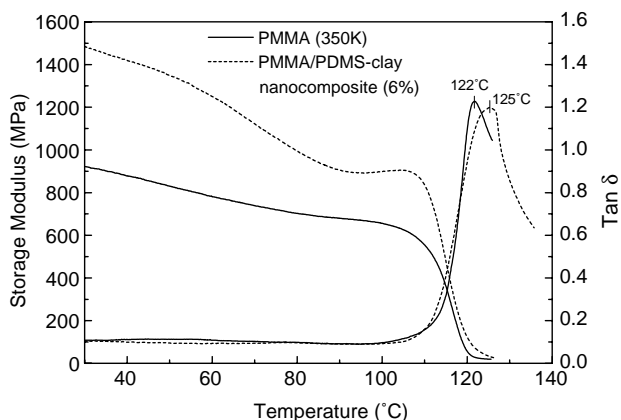
References

[1] LeBaron PC, Wang Z, Pinnavaia TJ. Appl Clay Sci 1999;15(1-2):11–29.

[2] Kojima Y, Usuki A, Kawasumi M, Okada A, Kurauchi T, Kamigaito O. J Polym Sci, Part A: Polym Chem 1993;31(4):983–6.

[3] Lee DC, Jang LW. J Appl Polym Sci 1996;61:1117–22.

[4] Zeng C, Lee LJ. Macromolecules 2001;34:4098–103.

[5] Wang D, Zhu J, Yao Q, Wilkie CA. Chem Mater 2002;14:3837–43.

[6] Shaffer KA, DeSimone JM. Trends Polym Sci 1995;3(5):146–53.

[7] DeSimone JM, Maury EE, Menceloglu YZ, McClain JB, Romack TJ, Combes JR. Science 1994;265(5170):356–9.

[8] Canelas DA, DeSimone JM. Macromolecules 1997;30:5673–82.

[9] Hems WP, Yong TM, van Nunen JLM, Cooper AI, Holmes AB, Griffin DA. J Mater Chem 1999;9(7):1403–7.

[10] Lepilleur C, Beckman EJ. Macromolecules 1997;30:745–56.

[11] Shaffer KA, Jones TA, Canelas DA, DeSimone JM, Wilkinson SP. Macromolecules 1996;29:2704–6.

[12] Christian P, Howdle SM, Irvine DJ. Macromolecules 2000;33:237–9.

[13] Zerda A, Caskey T, Lesser A. Macromolecules 2003;36:1603–8.

[14] Dong Z, Liu Z, Zhang J, Han B, Sun D, Wang Y, et al. J Appl Polym Sci 2004;94:1194–7.

[15] Zhao Q, Samulski E. Macromolecules 2005;38:7967–71.

[16] Chou CC, Chang YC, Chiang ML, Lin JJ. Macromolecules 2004;37:473–7.

[17] Okubo M, Fujii S, Minami H. Progr Colloid Polym Sci 2004;124:121–5.

[18] McHugh M, Krukonis V. Supercritical fluid extraction. 2nd ed. Washington: Butterworth-Heinemann; 1994.

[19] Shiho H, DeSimone JM. J Polym Sci, Part A: Polym Chem 2000;38:1146–53.

[20] Shiho H, DeSimone JM. J Polym Sci, Part A: Polym Chem 1999;37:2429–37.

[21] Kashiwagi T, Inaba A, Brown JE, Hatada K, Kitayama T, Masuda E. Macromolecules 1986;19:2160–8.

[22] Okamoto M, Morita S, Taguchi H, Kim Y, Kotaka T, Tateyama H. Polymer 2000;41:3887–90.

[23] McNally T, Murphy WR, Lew C, Turner R, Brennan G. Polymer 2003;44:2761–72.

[24] Xie W, Hwu JM, Jiang GJ, Buthelezi TM, Pan W-P. Polym Eng Sci 2003;43(1):214–22.